CHAPTER IV

Molecular Encapsulation Study of Indole-3-methanol in Cyclodextrins : Effect on Antimicrobial Activity and Cytotoxicity

Abstract : We investigated the encapsulation of indole-3-methanol (IM) within the nanocage of β-cyclodextrin (β-CD) and hydroxypropyl-β-cyclodextrin (HP-β-CD). The formation of encapsulated complexes have been confirmed by the experimental studies such as UV-Visible, Fluorescence, ^{1}H NMR, DSC, SEM, surface tension, FT-IR and mass spectrometry. DSC study revealed that the inclusion into CDs can enhance the thermal stability of IM. Molecular docking studies provided useful insight on the encapsulation mode of IM molecule into the cavity of CDs. The antimicrobial activity of IM was considerably improved after encapsulation. Further, the encapsulated complexes expressed low cytotoxic effect than free IM on the normal liver cell line WRL-68.

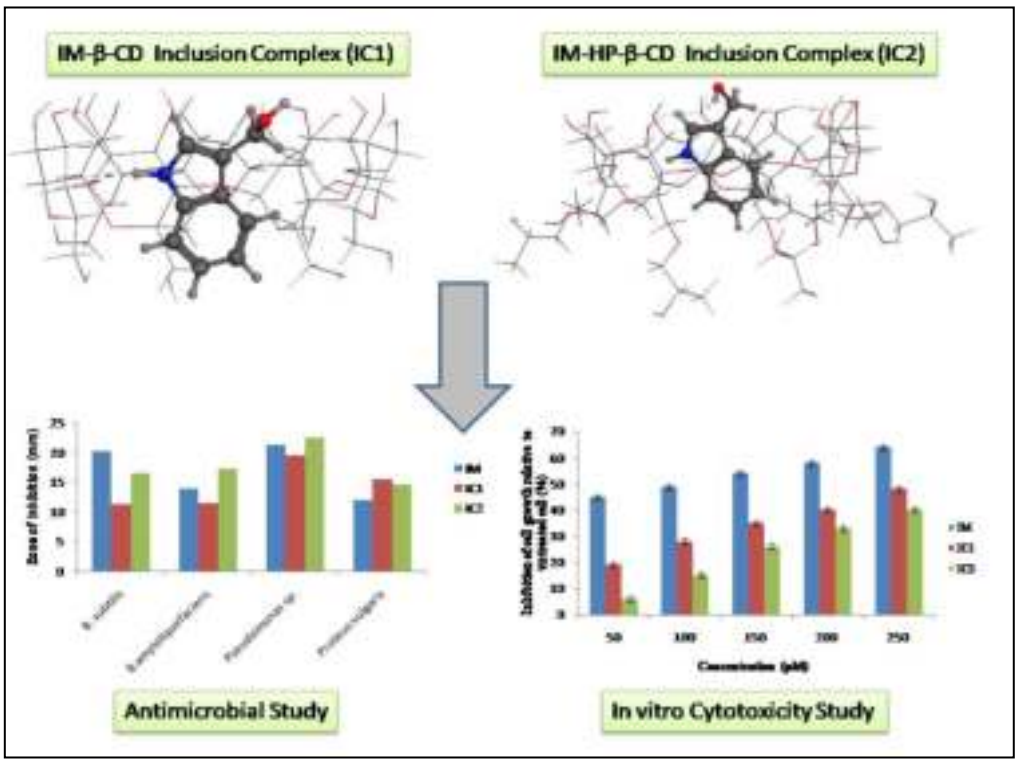

Keywords : Indole-3-methanol ; β-Cyclodextrin ; Hydroxypropyl-β-Cyclodextrin ; Molecular docking ; *In vitro* biological activity study.

IV.1. Introduction

In supramolecular chemistry, cyclodextrins (CDs) are interesting ideal host molecules.[1] They are cyclic oligosaccharides composed of six (α-CD), seven (β-CD & HP-β-CD) and eight (γ-CD) glucopyranose units linked by α-1,4-linkages with a hydrophobic cavity and a hydrophilic external surface.[2,3] They can form host–guest complexes by encapsulation of various organic, biological and pharmacological guest molecules into their internal hydrophobic cavity.[4,5] This usually enhances the chemical stability, solubility and bioavailability of the drug molecule.[6-11] Due to this interesting property, CDs have been used as drug carriers,[12-14] photochemical sensors,[15] enzyme mimics,[16] and separation reagents,[17] etc. CDs have been extensively exploited as excellent receptors and also applied to build stimuli-responsive supramolecular materials.[18] Inclusion with CD is the best way for the advancement of drug molecule's physicochemical properties.[19] The discharge of guest molecules from the ICs can be achieved by applying different external stimuli, such as, temperature, competitive binding, photosensing, enzyme activation and changes in pH.[20-23]

Indole-3-methanol (IM) is a phytochemical compound obtained from hydrolysis of glucosinolate glucobrassicin catalyzed by myrosinase. A comparatively high level of IM can be found in vegetables of the Brassica genus.[24] IM has been examined concerning important role in cancer management.[24-26] In human melanoma cells, IM result in proliferation arrest and apoptosis.[27] In situ and in vivo studies identifies a role of IM in breast and prostate cancer as a chemoprotective agent.[28] The anti-inflammatory effect of IM was also described.[29,30] These findings have showed that IM exhibits significant potential for biological purpose. However, in spite of its potential in pharmacology, IM is unstable to acidic environment, light and temperature changes,[31,32] which may restrict its broader applications in pharmaceutical science. Therefore, in order to retain or facilitate the biological activity of IM and enhance its stability from harsh environmental conditions, IM should be encapsulated in CDs forming host-guest ICs. Thus, CD can act as an encapsulating vehicle by forming IC for delivering the drug at the targeted site retaining its bioactivity.[11]

In our present work, we have studied the encapsulation of IM within the nanocage of β-CD and HP-β-CD. Job's plot and surface tension study have been used to explain the 1:1 encapsulation. We have employed the spectroscopic method to evaluate

association constant along with thermodynamic parameters. The ICs have been prepared and characterized by Fourier Transform Infrared (FT-IR) spectroscopy, High-Resolution Mass spectrometry (HRMS), ^{1}H Nuclear Magnetic Resonance (^{1}H NMR) spectroscopy, Differential Scanning Calorimetry and Scanning Electron Microscopy (SEM). Molecular modeling technique was utilized to get an insight into the possible interaction between IM and β-CD or HP-β-CD. Moreover, the antimicrobial activity against some pathogenic bacteria and *in vitro* cytotoxic activity on normal liver cell line were tested out to investigate the benefits of IM encapsulation.

IV.2. Experimental section

IV.2.1. Materials

Indole-3-methanol with purity>98% and Hydroxypropyl-β-cyclodextrin were procured from TCI chemicals India Pvt. Ltd. β-Cyclodextrin with purity 98% was purchased from Sigma-Aldrich, India and used as received.

IV.2.2. Methods

UV-Visible spectra were obtained by Agilent 8453 UV-Visible spectrophotometer. The temperature of the cell was kept fixed by an automated thermostat.

Surface tension experiments were performed using a digital K9 Tensiometer (Kruss, Germany) at 298.15K with the accuracy of ±0.1 mNm^{-1}.

Fluorescence spectra were taken by PTI QuantaMaster Fluorescence spectrophotometer, at 298K in a Hellma quartz cuvette.

^{1}H NMR measurements were carried out in DMSO-d_6 using Bruker Avance 300 MHz NMR spectrometer at 298.15 K.

HRMS spectra were recorded with positive-mode electrospray ionization in high-resolution Q-TOF instrument.

IR spectra were obtained by KBr disk method at room temperature on a Perkin-Elmer FTIR spectrometer.

Thermal analysis was performed in the temperature range of 30-300^{0}C under nitrogen gas atmosphere (1.5 atm.) on Perkin Elmer DSC-6 thermal analyzer.

Microscopic morphological structure analysis was carried out with JSM-6360 Scanning Electron Microscope (SEM).

IV.2.3. Molecular modeling study

The possible binding mode as well as binding affinity of IM with β-CD and HP-β-CD was simulated by employing MOE2015 software. The 3D optimized structures of IM and β-CD were extracted from Cambridge Crystal Data Centre (CCDC) as CIF file and used as received. The structure of HP-β-CD was constructed by MOE Builder function by attaching seven hydroxypropyl substituents in 2-position of β-CD. Energy minimization of HP-β-CD was performed using MOE QuickPrep protocol. The MOE2015 software available in the Chemical Computing Group (CCG) was used to dock the guest molecule IM into the cavity of β-CD and HP-β-CD. Molecular modeling calculations were performed with molecular mechanics MMFF94x force field. The charges and hydrogens were kept fixed, and the root mean square (RMS) gradient was put to 0.005 kcal/mol. The Triangle Matcher method and the London ΔG scoring function were used respectively for fitting and ranking the ligand (cyclodextrins) conformations. Based on the docking scores, the produced poses were given rank. Finally, the inclusion complex was opted according to the optimum scoring pose and docking energy.[33,34]

IV.2.4. Antimicrobial activity assay

The antimicrobial activity of pure IM along with its inclusion complexes [IM-β-CD (IC1) and IM-HP-β-CD (IC2)] has been studied using the agar well diffusion technique. Bacterial cultures of *Bacillus subtilis, Bacillus amyloliquefaciens, Pseudomonas* sp. and *Proteus vulgaris*, grown overnight at 37°C were spread over the nutrient agar plates. Using a sterile cork-borer, wells were made in the plates. To these wells, 40µl of DMSO as a control and 40µl 5mM DMSO solutions of IM and its complexes were added. The plates were incubated at 24 hours at 37°C. The solvent DMSO used to dissolve IM and its complexes, was kept as a control. Following the incubation, the zone of inhibition was computed.[35,36]

IV.2.5. *In vitro* cytotoxicity assay with normal cell line WRL-68

The cytotoxic activity of the compound IM and its inclusion complexes [IM-β-CD (IC1), IM-HP-β-CD (IC2)], against the normal cell line were resolved by employing the 3-(4,5-dimethylthiazol-2-yl)-2,5-diphenyl tetrazolium bromide (MTT) colorimetric assay. To initiate the assay, sterilized Dulbecco's Modified Eagle media was taken in a 100mm petridish and inoculated with the normal liver cell line (WRL-68). This media was also

enriched by the addition of 5% fetal bovine serum (FBS), antibiotics such as penicillin (100 IU/ml) and streptomycin (100 µg/ml) and incubated at 37˚C in a CO_2(5%) humidified incubator. To a 96 welled microtiter plates, 100 µl each of the cell culture at a concentration of 1×10^5 cells/ml were added and incubated in a CO_2 humidified incubator, temperature set to 37°C for 24 hours. Following incubation, the cells in each wells were subjected to treatment with varying concentrations of 5µl DMSO solutions of IM and its complexes. Past 24 hours of incubation in a 37°C set CO_2 incubator, the media in the wells of the microtiter plate was replaced with fresh medium and thereafter 10µl from the working solution of MTT (5mg/ml in phosphate buffer) was introduced to the wells. This was followed by the incubation of the microplate for 4 hours at 37°C set CO_2 incubator. The medium was subjected to aspiration and the formazan crystals formed in each wells of the microplate were dissolved using 50µl isopropanol. The degree to which the MTT was reduced to formazan crystals was assessed by computing the absorbance at 540 nm with the help of a microplate reader (Spectrostar nano, BMG Labtech). Lastly, the percentage of inhibition was computed by the formula; $(A_u-A_t/A_u)\times100$, where A_u means the control's (cells subjected to DMSO treatment) average absorbance value and A_t means the average absorbance value of the cells subjected to the treatment with IM and its inclusion complexes. The stock solutions of IM and its inclusion complexes were prepared using DMSO and also the final dilutions (to the desired concentrations) were made in DMSO.

IV.2.6. Preparation of inclusion complex

The two solid ICs [IC1 (IM-β-CD) and IC2 (IM-HP-β-CD)] have been prepared by mixing IM and CD in 1:1 molar ratio. 1.0 mmol CD was dissolved in 25 mL distilled water. Then predissolved 1.0 mmol IM in acetonitrile (AcN) [25 mL] was added slowly to an aqueous CD solution. This mixed solution was then kept at 48-50^{0}C with continuous stirring for 36 hours. The stirred solution`was filtered and then stored into refrigerator for 24 hours. The obtained suspension was filtered followed by drying in an oven at 70^{0}C for 9 hours. Finally, the solid inclusion powder was collected and preserved in dessicator for latter use.

IV.3. Result and Discussion

IV.3.1. Job plot determines the stoichiometry of the inclusion complex

In order to get an idea about the stoichiometry of the ICs a popularly known Job's method was applied using UV-Visible spectroscopic technique.[37] Job plots were obtained by plotting ΔA×R against R (where ΔA denotes the difference in absorbance of IM in absence and presence of CD, and R = [IM]/([IM] + [CD]). The solutions were prepared taking 1:5 (V:V) AcN:H_2O as solvent because of the poor water solubility of IM. Absorption maximum values were obtained at λ_{max}= 279 nm for a series of solutions in such a manner that the overall concentration, [IM] + [CD], remains fixed with varying mole fraction of IM in the range of 0-1 at 298.15 K (Tables 1 and 2). The maximum R value on the plot gives the stoichiometry of the complexation. In our present work, for both the systems IM-β-CD and IM-HP-β-CD, the observed maxima at R=0.5 clearly indicates 1:1 stoichiometric ratio of the ICs (Figure 1).[38]

IV.3.2. Surface tension study demonstrates the inclusion and stoichiometric ratio

The formation of host-guest IC and its stoichiometry can be evaluated by surface tension (γ) study.[39-41] In this study, IM and CDs solutions were prepared taking 1:5 (V:V) AcN:H_2O as solvent because of the poor water solubility of IM. IM solution was found to have lower surface tension than the pure 1:5 (V:V) AcN:H_2O suggesting that IM is surface active, which may be ascribed to the presence of a hydrophobic indole moiety and a carbinol (-CH_2OH) group.[42,43] While CDs, having hydrophilic rims and hydrophobic external surface (Scheme 1), does not display any alteration in γ of 1:5 (V:V) AcN:H_2O when dissolved in it in a significant range of concentration.[44,45] In our surface tension study, γ of IM solution were found to increase with increasing concentration of both β- and HP-β-CD (Tables 3 and 4, Figure 2) indicating the inclusion of surface-active IM molecules into the central hydrophobic cavity of CD molecules from the surface of the solution forming ICs (Scheme 2).[46] There was appearance of a break point in both the plots suggesting the formation of IC and also its 1:1 stoichiometry (Figure 2).[39,40] The concentrations of IM and CDs at each break point with corresponding γ values are listed in Table 5. The break points were observed at certain concentration where the molar concentration ratio of host CD and guest IM molecule are nearly 1:1. [46,43]

IV.3.3. Stability constants and thermodynamic parameters

The binding affinity of IM with β- and HP-β-CD can be determined by measuring association constant or stability constant (K_a) using UV-Visible spectroscopy.[46] For spectral measurement, 1:5 (V:V) AcN:H_2O was used as solvent because of the poor water solubility of IM. When IM molecules are encapsulated into the hydrophobic cavity of CD molecules, the environment of IM changes which results in the changes of molar extinction coefficient (ε).[47,48] The change in absorbance (ΔA) of IM was checked out at the temperature range 298.15 K to 308.15 K by varying the concentration of β- and HP-β-CD (Tables 6 and 7).[42] Based on Benesi-Hildebrand method for 1:1 complexes, the double reciprocal plots are drawn to calculate the K_a value using the following equation (Figure 3)[49,38]

$$\frac{1}{\Delta A} = \frac{1}{\Delta\varepsilon[IM]K_a}\frac{1}{[CD]} + \frac{1}{\Delta\varepsilon[IM]} \qquad (1)$$

where ΔA denotes the difference in absorbance of IM in absence and presence of CD. [IM] is the concentration of IM. The values of K_a for both IM-β-CD and IM-HP-β-CD ICs are determined from intercept/slope of the plots using equation 1 (Table 8).[50,46,42] The smaller K_a value of IM-β-CD (≃4.33 x 10^3 M^{-1} at 298.15 K) compared to that of IM-HP-β-CD (≃17.60 x 10^3 M^{-1} at 298.15 K) reveals that the binding capacity of β-CD is lower than HP-β-CD. This could be due to the steric hindrance induced by the substituted hydroxypropyl groups in HP-β-CD, which may lead to the widening of the cavity of HP-β-CD compared to that of β-CD.

The thermodynamic parameters ΔG^0, ΔS^0 and ΔH^0 can be obtained for the formation of inclusion complex from van't Hoff equation using values of K_a found at different temperatures.

$$\ln K_a = -\frac{\Delta H^o}{RT} + \frac{\Delta S^o}{R} \qquad (2)$$

The above linear equation involving $\ln K_a$ versus 1/T (Figure 4) provides the value of ΔH^0, ΔS^0 and ΔG^0 for the formation of ICs (Table 9). [51,42,48] The changes in enthalpy, entropy and free energy were found to be negative, positive and negative, indicating that the encapsulation process is exothermic, entropy-driven and spontaneous respectively. The large increase in entropy may be attributed to the release of highly ordered and restricted hydrogen-bonded water molecules in the direct

vicinity of hydrophobic component of the drug or inside the CDs into the bulk water during encapsulation of IM into CDs.[52] Therefore, the negative ΔH^0, positive ΔS^0 and negative ΔG^0 values reveals that the overall encapsulation process is thermodynamically favourable.

IV.3.4. Fluorescence study : Modified Benesi-Hildebrand equation and stability constants

The stability constants (K_a^F) of ICs can also be derived from the spectrofluorometric data using modified Benesi–Hildebrand equation.[53-55] A 1:5 (V:V) AcN:H_2O was used as solvent for spectral measurement because of the poor water solubility of IM. The K_a^F values obtained from fluorescence study are found in good agreement with that obtained from the UV-Visible spectroscopic study (Table 8). It was observed that there was enhancement of fluorescence intensities of IM (at λ_{max} = 358 nm) with increasing concentration of CDs (Tables 10 and 11) suggesting an encapsulation of IM molecule into an apolar cavity of CDs. Such enhancement in the intensities may be attributed to the screening of the excited singlet state of fluorophore with the apolar cavity of the CDs.[56,57] The stability constants (K_a^F) of ICs have been obtained using double reciprocal plots :

$$\frac{1}{F-F_o} = \frac{1}{(F_\infty - F_o)K_a^F}\frac{1}{[CD]} + \frac{1}{F_\infty - F_o} \qquad (3)$$

where F and F_0 represents the fluorescence intensities of IM with and without CDs respectively, F_∞ is the fluorescence intensity of completely complexed IM and K_a^F is the stability constant of IC.

Plots of $1/(F - F_o)$ against 1/[CD] showed a good linear relationship suggesting 1:1 complexation (Figure 5). The stability constants (K_a^F) of IM-β-CD and IM-HP-β-CD ICs, evaluated by the intercept/slope, were found to be 5.18 x 10^3 M^{-1} and 21.98 x 10^3 M^{-1} respectively at 298.15 K, which are in good agreement with that determined by the UV-Visible spectroscopic study (Table 8).

IV.3.5. ^{1}H NMR spectral analysis

^{1}H NMR is a powerful tool in studying solid ICs, which provides quantitative information on the possible inclusion mode of ICs.[58,59] The encapsulation of a guest into

a CD cavity causes changes in the chemical shift (δ) values of the guest as well as CD protons.[60] Usually the guest protons undergoes upfield chemical shifts upon inclusion into a CD cavity indicating that the protons of guest molecule were enclosed by electron density of the CDs.[61,62] The upfield shifts of the CD protons may also be observed owing to the induced anisotropic magnetic shielding produced by the encapsulated aromatic moiety of guest molecule.[63,64] In CD, H5 and H3 protons are situated in the interior of the cavity with H5 nearer to the narrower side and H3 to the wider side, whereas H4, H2 and H1 protons are placed at the outer surface (Scheme 1).[65,66] In the present work, the molecular encapsulation of IM with β- and HP-β-CD has been explored using ^{1}H-NMR spectroscopy. The NMR signals of IM protons and H5, H3 protons of β- and HP-β-CD were shown in Figures 6, 7 with their corresponding values of δ in Table 12. In case of solid ICs [IC1 (IM-β-CD) and IC2 (IM-HP-β-CD)], the NMR signals of the internal H5, H3 protons of β-CD and HP-β-CD along with the NMR signals of IM protons exhibited considerable upfield shifts, which confirms that IM is included inside the cavity of β- and HP-β-CD (Figures 6 and 7).[67] Looking at these chemical shifts, we can also notice that the H3 proton undergoes significantly higher upfield shift compared to H5 proton (Table 12), indicating the preferential insertion of the aromatic moiety of IM into the cavity of both β- and HP-β-CD from the wider rim (Scheme 2).[68]

IV.3.6. High resolution mass spectrometric analysis

The solid ICs were analyzed using high resolution mass spectrometry (HRMS). The peaks observed in the spectra shown in Figure 8 with their corresponding m/z values are listed in Table 13. The observed peaks with m/z values 1305.13, 1283.11, 1711.33 and 1689.42 corresponds to the molecular ions $[IM+β\text{-}CD+Na]^+$, $[IM+β\text{-}CD+H]^+$, $[IM+HP\text{-}β\text{-}CD+Na]^+$ and $[IM+HP\text{-}β\text{-}CD+H]^+$ respectively. The appearance of these distinct peaks supports the formation of the ICs, IM-β-CD and IM-HP-β-CD, and their stoichiometric ratio should be 1:1 (Scheme 2)[69,70] which is in accordance with the Job's method and surface tension study.

IV.3.7. FT-IR spectral analysis

FT-IR study was performed to examine the characteristic changes in the IR spectra supporting the formation of ICs of IM with β- and HP-β-CD.[71,67] The spectra are

shown in Figures 9 and 10, and the vibrational frequencies with their corresponding chemical bonds have been set into Table 14.

The following changes in the IR spectra were observed for IM-β-CD IC (Figure 9) : The stretching vibrations involving O-H/N-H groups of IM at 3390 cm^{-1} and that of O-H of β-CD at 3387 cm^{-1} were appeared at 3409 cm^{-1} as a broad peak in the IC. The aromatic C=C skeletal stretching vibrations in IM were found to appear at 1616, 1551, 1455 cm^{-1}, and the aromatic C-H bending vibrations were observed at 1250 cm^{-1} (in-plane) and 744, 832 cm^{-1} (out-of-plane). Such C-H bending vibrations for IC were shifted to 1237 cm^{-1} (in-plane) and 747, 844 cm^{-1}(out-of-plane), along with disappearance of aromatic skeletal C=C stretching vibrations. The observed alteration of C-H bending modes and the disappearance of aromatic C=C skeletal stretching vibrations in IC indicates the encapsulation of aromatic indole moiety into the β-CD cavity with restriction of some modes of vibration of the IM within the cavity. The C-H bending modes were appeared at 1408, 1362, 1339 cm^{-1} for β-CD, and these bending modes were found to shift at 1392 cm^{-1}, which may be due to the close proximity of aromatic moiety of IM.

Similarly, the following IR spectral shifts were observed for IM-HP-β-CD IC (Figure 10) : The stretching vibrations involving O-H/N-H groups of IM at 3390 cm^{-1} and that of O-H of HP-β-CD at 3411 cm^{-1} were appeared at 3396 cm^{-1} as a broad peak in the IC. The aromatic C=C skeletal stretching vibrations in pure IM were observed at 1616, 1551, 1455 cm^{-1}, and the aromatic C-H bending vibrations were noticed at 1250 cm^{-1} (in-plane) and 744, 832 cm^{-1} (out-of-plane). These C-H bending vibrations for IC were shifted to 1243 cm^{-1} (in-plane) and 748, 844 cm^{-1}(out-of-plane), along with appearance of only one skeletal stretching vibration involving aromatic C=C at 1455 cm^{-1}. The observed shifts of C-H bending modes and the disappearance of other two aromatic C=C skeletal stretching vibrations (1616 and 1551 cm^{-1}) in IC suggest the encapsulation of aromatic indole ring into the HP-β-CD cavity with restriction of some vibrational modes of the IM within the host cavity. The C-H bending frequency of HP-β-CD at 1375 cm^{-1} was found to shift at 1367 cm^{-1} for IC, which may be due to the close proximity of aromatic moiety of IM.

All these observations suggest that the appearance of shifting in IR spectra indicates the formation of IM-β-CD and IM-HP-β-CD ICs. Thus the results observed from FTIR study are in good correlation with the results of ^{1}H NMR.

IV.3.8. DSC analysis

The differential scanning calorimetry (DSC) analysis was further utilized to provide additional evidence for the formation of inclusion complexes. The DSC curve of IM showed a sharp endothermic peak at 98^{0}C, which corresponds to its melting point. Broader endothermal peaks provided with water loss for β-CD around 101^{0}C and HP-β-CD around 85^{0}C were registered. However, there was disappearance of endothermic peak at about 98^{0}C corresponding to the pure IM in the DSC thermograms of complexes, and the appearance of a new endothermic peak with a lower intensity at 106^{0}C and 115^{0}C for IM-β-CD and IM-HP-β-CD complexes respectively, were encountered (Figures 11 and 12). These outcomes not only confirm the formation of inclusion complexes, but also suggest that these inclusion complexes are comparatively stable than the pure IM from a thermal point of view.

IV.3.9. SEM technique : Surface morphology analysis

The surface morphological studies of solid samples can be carried out by scanning electron microscopy (SEM).[72,73] The SEM image analysis provides an additional evidence in support of the formation of ICs of IM with β- and HP-β-CD. The surface morphology of IM, HP-β-CD, its physical mixture (PM2) and solid inclusion complex (IC2) are shown in Figure 13(A). HP-β-CD consisted of round amorphous particle with aperture on its surface, and IM showed a group of plate shaped crystal in an aggregated form. Particles of HP-β-CD were found on the surface of IM in case of physical mixture. In contrast, inclusion complex was found to appear as irregular shaped crystal with a significant change in the morphology and crystalline nature. Similarly, the surface morphology of IM, β-CD, its physical mixture (PM1) and inclusion complex (IC1) are presented in Figure 13(B). In β-CD, the particles were observed as uneven cubic crystal with large dimensions. The physical mixture displayed some similarities with the free components and has morphology comparable with these pure components. However, the particles of solid complex appeared as tiny flakes with a drastic change in the morphological structure and crystalline nature. These results

confirms the formation of the inclusion complexes of IM with β- and HP-β-CD, i.e., IM-β-CD (IC1) and IM-HP-β-CD (IC2).

IV.3.10. Molecular docking studies

Molecular docking studies were implemented to come up with useful insight on the encapsulation mode of guest molecule into the cavity of CD in previous literatures, which may aid the experimental estimations.[74-76,82] In this study, Molecular Operating Environment (MOE) docking method was used to explore the 3-D supramolecular structures of inclusion complexes, IM-β-CD (IC1) and IM-HP-β-CD (IC2). On the basis of the outcome of Job's method, surface tension study and HRMS analysis, a 1:1 stoichiometry of IM and the CDs was selected for molecular docking. The best docked conformation of IC1 (a, side view; b, top view) and IC2 (c, side view; d, top view) are presented in Figure 14. The previous literature[77] reports the inclusion of the indole ring of 3-substituted indole derivatives through the wider rim of β-CD. There are also literature[78] based on molecular modeling which reports the inclusion of the hydrocarbon chain of 3H-indole derivatives within the β-CD cavity through the wider rim and the enhancement of complex stability or binding ability with the increase in the length of alkyl chain. However, in our present work, the observed ^{1}H NMR and IR spectral shifts suggested the entrance of indole moiety from the benzene ring side of IM into the hydrophobic cavity of β- and HP-β-CD rather than the entrance from polar $-CH_2OH$ side of IM, which is in agreement with our findings from docking. Based on our docking study, the inclusion or binding mode of indole moiety through the wider side of β- and HP-β-CD cavity can be accounted by the fact that the indole ring being more hydrophobic than the small hydrophilic carbinol ($-CH_2OH$) group, the probable inclusion occurs from the benzene ring side of IM with carbinol group surrounded by hydrophilic secondary -OH group network near the wider rim. Further, molecular docking indicates that the additional H-bonding interaction of pyrrole –NH group with glucoside ether linkage in docked conformation of IM-β-CD (IC1) and the similar type of interaction of carbinol –OH group with secondary -OH group in docked conformation of IM-HP-β-CD (IC2) provides more stability with better binding to the ICs (Figure 14), which is clearly reflected from the binding constant values of IC1 ($\simeq 4.33 \times 10^3$ M^{-1}) and IC2 ($\simeq 17.60 \times 10^3$ M^{-1}) obtained from UV-Visible spectroscopic studies. The binding energy of IC2 (- 19.25 kJ mol^{-1}) was found to be lower than that of IC1 (- 17.15 kJ

mol^{-1}) [Table 15], which indicates that the substitution of hydroxypropyl group improved the inclusion capacity of β-CD, as determined by the UV-Visible spectroscopic studies. This could be probably attributed to the extension of the size of β-CD cavity on derivatization with hydroxypropyl group, which makes IM penetrate conveniently into the cavity improving complex forming ability.[79,80]

IV.3.11. *In vitro* biological activity study

IV.3.11.1. Antimicrobial activity

About 70% of death cases have been found to be caused by bacterial infections.[81] In the present work, we have analyzed IM and its inclusion complexes IC1 and IC2 for their antimicrobial efficiency against some pathogenic bacteria.

The antibacterial effect has been examined taking four different bacteria, namely, *Proteus vulgaris, Pseudomonas sp., Bacillus amyloliquefaciens* and *Bacillus subtilis* by agar well diffusion technique (Figures 15 and 16). The results listed in Table 16 showed that the IM and its complexes possesses antibacterial effect against gram-positive as well as gram-negative pathogenic bacteria. IC2 showed relatively greater inhibitory effect than free IM against *B. amyloliquefaciens*, *Pseudomonas sp.* and *P. vulgaris*, with 54, 51 and 45% inhibition respectively, whereas IC1 had greater inhibitory effect of 49% than pure IM against *P. vulgaris* only. The IM and its inclusion complexes inhibited the growth of bacterial cultures irrespective of their gram nature. Ultimately this relative study confers that the inclusion complexes displayed fairly better antibacterial efficacy than pure IM, which probably may be due to the ability of CDs to release the IM readily from the ICs or due to the increase of solubility of IM after complexation. However, IC2 provided greater activity than IC1.

IV.3.11.2. *In vitro* cyctotoxic activity

The cytotoxicity of pure IM, IM-β-CD (IC1) and IM-HP-β-CD (IC2) complexes has been investigated by exposing normal liver cell line WRL-68 to a series of five sets of free IM, IC1 and IC2 with each set having different concentrations (50, 100, 150, 200, 250 μM), and the cell viability was analyzed by means of an MTT assay. From Figure 17(a,b), it can be seen that for each of the five sets, IC1 and IC2 complexes showed lower cytotoxicity or lower percentage inhibition than pure IM. The mean concentration of IC1

and IC2 that caused 50 % cell inhibition was increased to 264 and 301 μM respectively compared with 107 μM of free IM (Table 17). Interestingly, these results suggested that IC1 and IC2 inhibits the cell growth of tested cells minorly than free IM, showing inclusion complexes of IM to be less cytotoxic than pure IM. This may be probably due to the fact that the sustained release of IM from inclusion complexes makes IM less exposed to the cell, which may result in low endocytic uptake of IM from the inclusion complex compared to the pure IM.[82,83]

IV.4. Conclusion

In this study, we report herein the supramolecular interactions of macrocyclic host (β-CD and HP-β-CD) with important phytochemical compound IM and formation of their ICs, which can be used in near future for an efficient regulatory delivery of IM retaining its bioactivity. The surface tension study and Job's method suggested the formation of mono-molecular encapsulated complex, which was further confirmed by mass spectral analysis. The stability constants and thermodynamic parameters determined from the reliable spectroscopic methods accounts for the stability of ICs formed and the thermodynamic feasibility of inclusion process respectively. The increase in ΔS^0 and a drop in ΔG^0 indicates the inclusion process to be thermodynamically favourable. The greater value of association constant, and hence more stability of IM-HP-β-CD IC compared to IM-β-CD IC is attributed to the larger cavity diameter of HP-β-CD than β-CD. FT-IR study and SEM image analysis confirmed the formation of IC from structural and morphological details. ^{1}H NMR spectroscopic analysis provided a deep insight towards the mode of complexation in which aromatic ring of IM was encapsulated from the wider rim side of the cavity of CDs. DSC study revealed that the inclusion into CDs can enhance the thermal stability of IM. The molecular docking simulation revealed the possible interaction of IM with β- and HP-β-CD giving stable 3-D structures of the ICs. The antimicrobial activity of IM was considerably improved after its encapsulation in CDs, however, IM-HP-β-CD IC provided better activity than IM-β-CD IC. Further, both IM-β-CD and IM-HP-β-CD ICs expressed low cytotoxic effect than free IM on the normal liver cell line WRL-68. Therefore, the encapsulation of IM into CDs can be a potential approach to improve stability and biological activity of IM for applications in the pharmaceutical industries and biomedical sciences.

Tables

Table 1. Data for the Job plot performed by UV-Visible spectroscopy for IM-β-CD system in 1:5 (V:V) acetonitrile-water at 298.15K[a]

IM (mL)	β-CD (mL)	IM (μM)	β-CD (μM)	[IM]/([IM]+[β-CD])	Absorbance (A)	ΔA	ΔA×[IM]/([IM]+[β-CD])
0.0	3.0	0	60	0.0	0.00000	0.41188	0.00000
0.3	2.7	6	54	0.1	0.01334	0.39854	0.03985
0.6	2.4	12	48	0.2	0.03525	0.37662	0.07532
0.9	2.1	18	42	0.3	0.10068	0.31120	0.09336
1.2	1.8	24	36	0.4	0.13537	0.27651	0.11060
1.5	1.5	30	30	0.5	0.17730	0.23458	0.11729
1.8	1.2	36	24	0.6	0.22008	0.19179	0.11507
2.1	0.9	42	18	0.7	0.26134	0.15053	0.10537
2.4	0.6	48	12	0.8	0.30584	0.10603	0.08483
2.7	0.3	54	6	0.9	0.35298	0.05889	0.05300
3.0	0.0	60	0	1.0	0.41188	0.00000	0.00000

[a]Standard uncertainties in temperature u are: u(T) = ±0.01 K.

Table 2. Data for the Job plot performed by UV-Visible spectroscopy for IM-HP-β-CD system in 1:5 (V:V) acetonitrile-water at 298.15K[a]

IM (mL)	HP-β-CD (mL)	IM (μM)	HP-β-CD (μM)	[IM]/ ([IM]+[HP-β-CD])	Absorbance (A)	ΔA	ΔA×[IM]/ ([IM]+[HP-β-CD])
0.0	3.0	0	60	0.0	0.00000	0.41188	0.000000
0.3	2.7	6	54	0.1	0.03902	0.37286	0.037286
0.6	2.4	12	48	0.2	0.07697	0.33491	0.066982
0.9	2.1	18	42	0.3	0.11346	0.29842	0.089526
1.2	1.8	24	36	0.4	0.16225	0.24963	0.099852
1.5	1.5	30	30	0.5	0.19222	0.21966	0.109830
1.8	1.2	36	24	0.6	0.24298	0.1689	0.101340
2.1	0.9	42	18	0.7	0.29083	0.12105	0.084735
2.4	0.6	48	12	0.8	0.3238	0.08808	0.070464
2.7	0.3	54	6	0.9	0.39009	0.02179	0.019611
3.0	0.0	60	0	1.0	0.41188	0.00000	0.000000

[a]Standard uncertainties in temperature u are: u(T) = ±0.01 K.

Table 3. Data for surface tension study of IM-β-CD system in 1:5 (V:V) acetonitrile-water at 298.15K[a]

Volume of β-CD (mL)	Total volume (mL)	Conc of IM (mM)	Conc of β-CD (mM)	Surface tension (mN m^{-1})

0	10	10.000	0.000	34.7
1	11	9.091	0.909	36.1
2	12	8.333	1.667	37.6
3	13	7.692	2.308	38.7
4	14	7.143	2.857	39.6
5	15	6.667	3.333	40.5
6	16	6.250	3.750	41.3
7	17	5.882	4.118	41.9
8	18	5.556	4.444	42.5
9	19	5.263	4.737	43.0
10	20	5.000	5.000	43.4
11	21	4.762	5.238	43.7
12	22	4.545	5.455	44.0
13	23	4.348	5.652	44.1
14	24	4.167	5.833	44.2
15	25	4.000	6.000	44.2
16	26	3.846	6.154	44.3
17	27	3.704	6.296	44.4
18	28	3.571	6.429	44.4
19	29	3.448	6.552	44.5
20	30	3.333	6.667	44.5

[a]Standard uncertainties in temperature u are: u(T) = ±0.01 K.

Table 4. Data for surface tension study of IM-HP-β-CD system in 1:5 (V:V) acetonitrile-water at 298.15K[a]

Volume of HP-β-CD (mL)	Total volume (mL)	Conc of IM (mM)	Conc of HP-β-CD (mM)	Surface tension (mN m^{-1})
0	10	10.000	0.000	34.7
1	11	9.091	0.909	36.5
2	12	8.333	1.667	38.0
3	13	7.692	2.308	39.2
4	14	7.143	2.857	40.3
5	15	6.667	3.333	41.2
6	16	6.250	3.75	42.0
7	17	5.882	4.118	42.7
8	18	5.556	4.444	43.2
9	19	5.263	4.737	43.4
10	20	5.000	5.000	43.5
11	21	4.762	5.238	43.6
12	22	4.545	5.455	43.7
13	23	4.348	5.652	43.8
14	24	4.167	5.833	43.8
15	25	4.000	6.000	43.9
16	26	3.846	6.154	43.9

17	27	3.704	6.296	43.9
18	28	3.571	6.429	44.0
19	29	3.448	6.552	44.0
20	30	3.333	6.667	44.1

[a]Standard uncertainties in temperature u are: u(T) = ±0.01 K.

Table 5. Surface tension (γ) values at the break point and the corresponding concentrations of CD and IM at 298.15 K[a]

	Conc. of IM (mM)	Conc. of CD (mM)	γ^a (mNm^{-1})
β-CD	4.55	5.45	44.0
HP-β-CD	5.56	4.44	43.2

Table 6. Data for the Benesi-Hildebrand double reciprocal plot performed by UV-Visible spectroscopy for IM-β-CD system in 1:5 (V:V) acetonitrile-water ; ± indicates the standard deviation

Temp (K[a])	IM (μM)	β-CD (mM)	A_o	A	1/[β-CD] (M^{-1})	1/ΔA	Intercept	Slope	K_a x 10^{-3} (M^{-1})
	50	0.5		0.31432	2000	24.83238			
	50	1.0		0.32143	1000	21.10595			
298.15	50	1.5	0.27405	0.32481	667	19.70055	17.04006	0.00394	4.33±0.17
	50	2.0		0.32552	500	19.42879			
	50	2.5		0.32823	400	18.45700			
	50	3.0		0.32951	333	18.03101			
	50	0.5		0.31293	2000	0.03888			
	50	1.0		0.32095	1000	0.0469			
303.15	50	1.5	0.27405	0.32386	667	0.04981	17.35089	0.00416	4.17±0.09
	50	2.0		0.32498	500	0.05093			
	50	2.5		0.32637	400	0.05232			
	50	3.0		0.32781	333	0.05376			
	50	0.5		0.31160	2000	0.03755			
	50	1.0		0.32015	1000	0.0461			
308.15	50	1.5	0.27405	0.32266	667	0.04861	17.71047	0.00438	4.04±0.12
	50	2.0		0.32398	500	0.04993			
	50	2.5		0.32547	400	0.05142			
	50	3.0		0.32571	333	0.05166			

[a]Standard uncertainties in temperature u are: u(T) = ±0.01 K.

Table 7. Data for the Benesi-Hildebrand double reciprocal plot performed by UV-Visible spectroscopy for IM-HP-β-CD system in 1:5 (V:V) acetonitrile-water ; ± indicates the standard deviation

Temp (K^a)	IM (μM)	HP-β-CD (mM)	A_o	A	1/[HP-β-CD] (M^{-1})	1/ΔA	Intercept	Slope	$K_a x10^{-3}$ (M^{-1})
	50	0.5		0.32412	2000	19.97204			
	50	1.0		0.32678	1000	18.96454			
298.15	50	1.5	0.27405	0.32737	667	18.75469	17.94768	0.00102	17.60±0.99
	50	2.0		0.32809	500	18.50481			
	50	2.5		0.32864	400	18.31837			
	50	3.0		0.32902	333	18.19174			
	50	0.5		0.32348	2000	20.23063			
	50	1.0		0.32614	1000	19.19754			
303.15	50	1.5	0.27405	0.32729	667	18.78287	18.09253	0.00108	16.75±0.47
	50	2.0		0.32753	500	18.69858			
	50	2.5		0.32812	400	18.49454			
	50	3.0		0.32834	333	18.41960			
	50	0.5		0.32288	2000	20.47921			
	50	1.0		0.32551	1000	19.43257			
308.15	50	1.5	0.27405	0.32659	667	19.03312	18.25839	0.00113	16.16±0.61
	50	2.0		0.32698	500	18.89288			
	50	2.5		0.32762	400	18.66716			
	50	3.0		0.32793	333	18.55976			

[a]Standard uncertainties in temperature u are: u(T) = ±0.01 K.

Table 8. Stability constant of different IM-CD inclusion complexes obtained from UV-Visible (K_a) and spectrofluorimetric data (K_a^F) using Benesi-Hildebrand method ; ± indicates the standard deviation

Guest	Host	Temperature(K^a)	K_a x 10^{-3} (M^{-1})	K_a^F x 10^{-3} (M^{-1})
IM	β-CD	298.15	4.33±0.17	5.18±0.24
		303.15	4.17±0.09	
		308.15	4.04±0.12	
Guest	Host	Temperature(K^a)	K_a x 10^{-3} (M^{-1})	K_a^F x 10^{-3} (M^{-1})
IM	HP-β-CD	298.15	17.60±0.99	21.98±1.42
		303.15	16.75±0.47	
		308.15	16.16±0.61	

Table 9. Data of the van't Hoff equation for calculation of thermodynamic parameters ΔH^0, ΔS^0 and ΔG^0 of IM-β-CD and IM-HP-β-CD inclusion complexes ; ± indicates the standard deviation

Host	T(K[a])	1/T	K_a $M^{-1}x10^{-3}$	$\ln K_a$	Slope	Intercept	ΔH^0 kJ mol^{-1}	ΔS^0 J mol^{-1} K^{-1}	ΔG^0 kJ mol^{-1}
β-CD	298.15	0.003356	4.325	8.37217	619.1	6.294	-5.15±0.17	52.33±0.57	-20.75±0.08
	303.15	0.003300	4.171	8.33591					
	308.15	0.003247	4.043	8.30474					
HP-β-CD	298.15	0.003356	17.596	9.77543	776.5	7.166	-6.46±0.23	59.57±0.76	-24.23±0.11
	303.15	0.003300	16.752	9.72627					
	308.15	0.003247	16.158	9.69017					

[a]Standard uncertainties in temperature u are: u(T) = ±0.01 K.

Table 10. Spectrofluorimetric data for the Benesi-Hildebrand double reciprocal plot of IM-β-CD system in 1:5 (V:V) acetonitrile-water at 298.15 K[a] ; ± indicates the standard deviation

IM (μM)	β-CD (mM)	F_o	F	$F-F_o$	1/[β-CD] (M^{-1})	1/ΔF $(x10^4)$	Intercept $(x10^4)$	Slope $(x10^8)$	$K_a^F x10^{-3}$ (M^{-1})
5.0	0.5	138696.9	144860.0	6163.122	2000	1.622554	1.17168	2.26403	5.18±0.24
	1.0		145887.1	7190.195	1000	1.390783			
	1.5		146173.1	7476.164	667	1.337584			
	2.0		146375.4	7678.445	500	1.302347			
	2.5		14660.02	7905.063	400	1.265012			
	3.0		146885.8	8188.852	333	1.221172			

[a]Standard uncertainties in temperature u are: u(T) = ±0.01 K.

Table 11. Spectrofluorimetric data for the Benesi-Hildebrand double reciprocal plot of IM-HP-β-CD system in 1:5 (V:V) acetonitrile-water at 298.15 K[a] ; ± indicates the standard deviation

IM (μM)	HP-β-CD (mM)	F_o	F	$F-F_o$	1/[α-CD] (M^{-1})	1/ΔF $(x10^4)$	Intercept $(x10^4)$	Slope $(x10^9)$	$K_a^F x10^{-3}$ (M^{-1})
5.0	0.5	138696.9	145662.0	6965.122	2000	1.43573	1.31863	5.99964	21.98±1.42
	1.0		145932.1	7235.195	1000	1.38213			
	1.5		146017.4	7320.476	667	1.36603			
	2.0		146102.7	7405.757	500	1.35030			
	2.5		146166.3	7469.375	400	1.33880			
	3.0		146200.1	7503.164	333	1.33277			

[a]Standard uncertainties in temperature u are: u(T) = ±0.01 K.

Table 12. ^{1}H NMR data of IM, β-CD, HP-β-CD and the solid inclusion complexes IM-β-CD (IC1) and IM-HP-β-CD (IC2) in DMSO-d_6. ND : not detected.

H protons	ppm (DMSO-d_6)			H protons	ppm (DMSO-d_6)		
	IM	β-CD	IM-β-CD (IC1)		IM	HP-β-CD	IM-HP-β-CD (IC2)
H2	7.23	–	7.19	H2	7.23	–	7.22
H6	7.58	–	7.52	H6	7.58	–	7.51
H7	6.97	–	6.89	H7	6.97	–	6.92
H8	7.08	–	7.03	H8	7.08	–	7.03
H9	7.34	–	7.32	H9	7.34	–	7.31
H2	–	3.42	3.41	H2	–	3.27	ND
H3	–	3.81	3.71	H3	–	3.84	3.71
H4	–	3.28	3.28	H4	–	3.15	ND
H5	–	3.63	3.58	H5	–	3.65	3.60

Table 13. The observed peaks at different m/z with corresponding ions for the solid inclusion complexes

IM-β-CD inclusion complex		IM-HP-β-CD inclusion complex	
m/z	Ion	m/z	Ion
148.09	$[IM+H]^+$	148.09	$[IM+H]^+$
1135.31	$[β\text{-}CD+H]^+$	1542.35	$[HP\text{-}β\text{-}CD+H]^+$
1283.14	$[IM+β\text{-}CD+H]^+$	1689.42	$[IM+HP\text{-}β\text{-}CD+H]^+$
1305.13	$[IM+β\text{-}CD+Na]^+$	1711.33	$[IM+HP\text{-}β\text{-}CD+Na]^+$

Table 14. FT-IR spectral frequencies of IM, β-CD, HP-β-CD and solid inclusion complexes

Indole-3-methanol	
Wavenumber /cm^{-1}	Group
3390	O-H stretching/N-H stretching
1616, 1551, 1455	Aromatic C=C stretching
1250	Aromatic in-plane C-H bending
744, 832	Aromatic out-of-plane C-H bending
1351	Aromatic C-N stretching

β-CD		HP-β-CD	
Wavenumber /cm^{-1}	Group	Wavenumber /cm^{-1}	Group
3387	O-H stretching	3411	O-H stretching
2925	C-H stretching	2926	C-H stretching
1408, 1362, 1339	C-H bending	1375	C-H bending
1156	C-O-C bending	1159	C-O-C bending
1031	C-C-O stretching	1035	C-C-O stretching
950	skeletal vibration involving α-1,4-linkage	949	skeletal vibration involving α-1,4-linkage

IM-β-CD inclusion complex		IM-HP-β-CD inclusion complex	
Wavenumber /cm^{-1}	Group	Wavenumber /cm^{-1}	Group
3409	O-H stretching/N-H stretching	3396	O-H stretching/N-H stretching
2929	C-H stretching	2928	C-H stretching
1237	Aromatic in-plane C-H bending	1459	Aromatic C=C stretching
747, 844	Aromatic out-of-plane C-H bending	1243	Aromatic in-plane C-H bending
1392	C-H bending	748, 844	Aromatic out-of-plane C-H bending
1026	C-C-O stretching	1367	C-H bending
949	skeletal vibration involving α-1,4-linkage	1031	C-C-O stretching
		944	skeletal vibration involving α-1,4-linkage

Table 15. Binding affinity of IM with β-CD and HP-β-CD derived from Molecular Docking

Ligand with receptor	Binding affinity(ΔG^0) in kJ mol^{-1}
IM-β-CD (IC1)	- 17.15
IM-HP-β-CD (IC2)	- 19.25

Table 16. Antimicrobial activity of pure IM, IM-β-CD (IC1) and IM-HP-β-CD (IC2) against different microbes

Microbes	Zone of inhibition (mm)		
	IM	IC1	IC2
B. subtilis	20.3	11.3	16.6
B.amyloliquefaciens	14.0	11.6	17.3
Pseudomonas sp.	21.3	19.6	22.6
Proteus vulgaris	12	15.6	14.6

Microbes	Percentage inhibition (%)		
	IM	IC1	IC2
B. subtilis	61.0	29.0	52.0
B.amyloliquefaciens	42.0	31.0	54.0
Pseudomonas sp.	48.0	44.0	51.0
Proteus vulgaris	33.3	49.0	45.0

Table 17. Values of "Half maximal inhibitory concentration" of pure IM, IM-β-CD (IC1) and IM-HP-β-CD (IC2)

	IM	IC1	IC2
Half maximal inhibitory concentration	107 µM	264 µM	301 µM

Figures

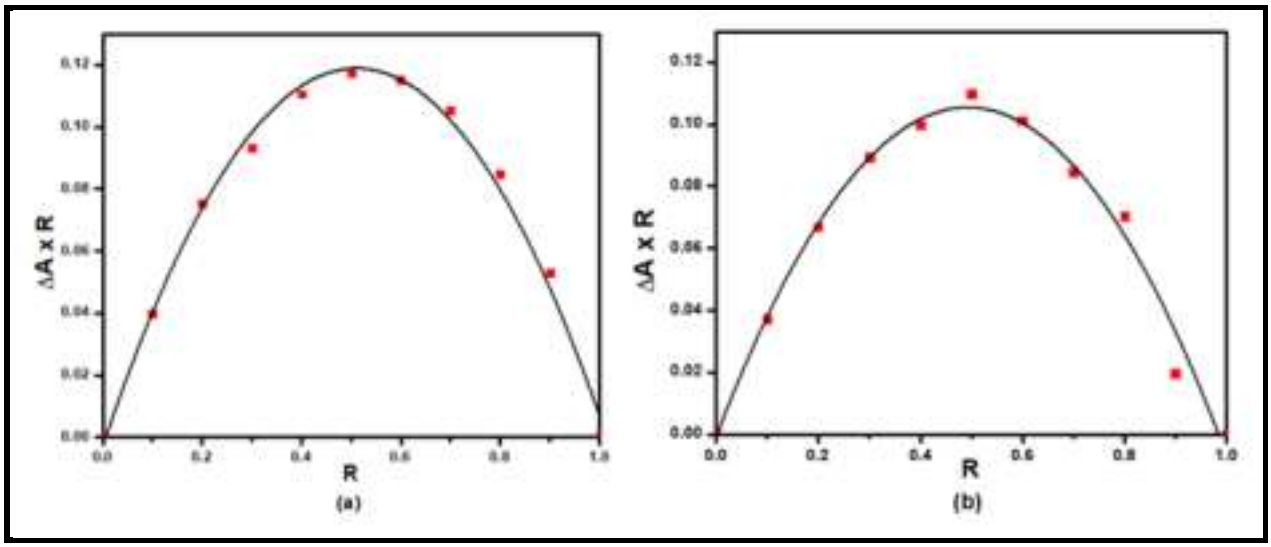

Figure 1. Job plots of the (a) IM-β-CD and (b) IM-HP-β-CD systems at 298.15 K in 1:5 (V:V) AcN:H_2O at λ_{max} = 279 nm. ΔA = difference in absorbance of IM in absence and presence of CD, R = [IM]/([IM] + [CD]).

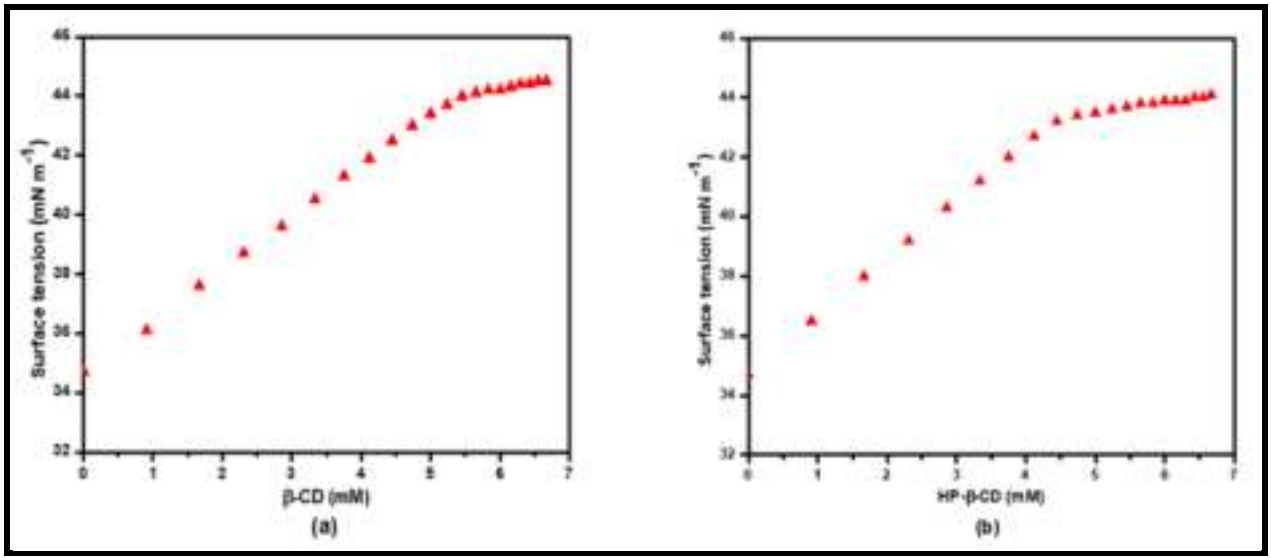

Figure 2. Variation of surface tension of (a) IM with increasing β-CD concentration and (b) IM with increasing HP-β-CD concentration at 298.15 K.

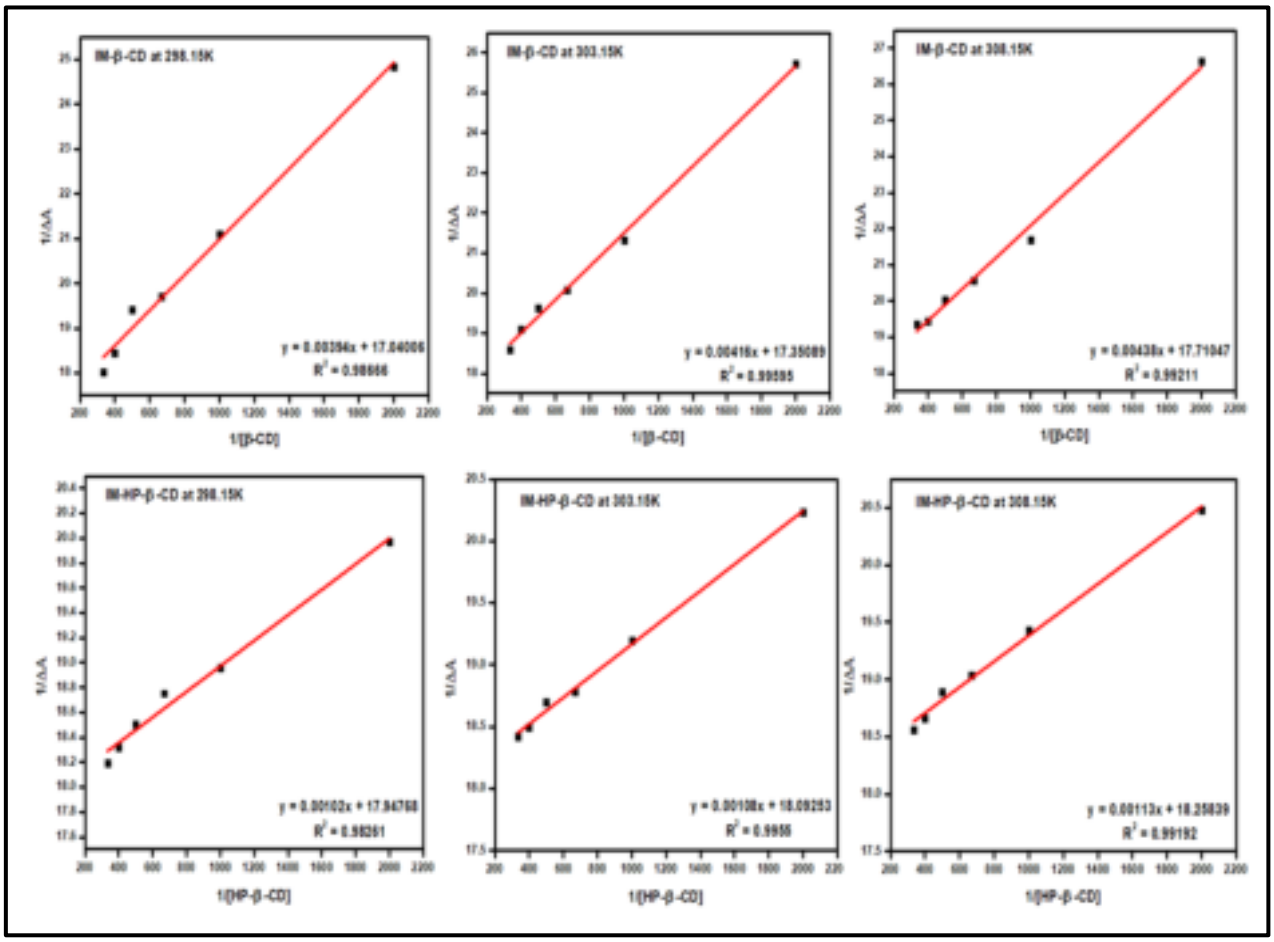

Figure 3. Benesi-Hildebrand double reciprocal plots for the effect of β-CD and HP-β-CD on the absorbance of IM (λ_{max} = 279 nm) at different temperatures.

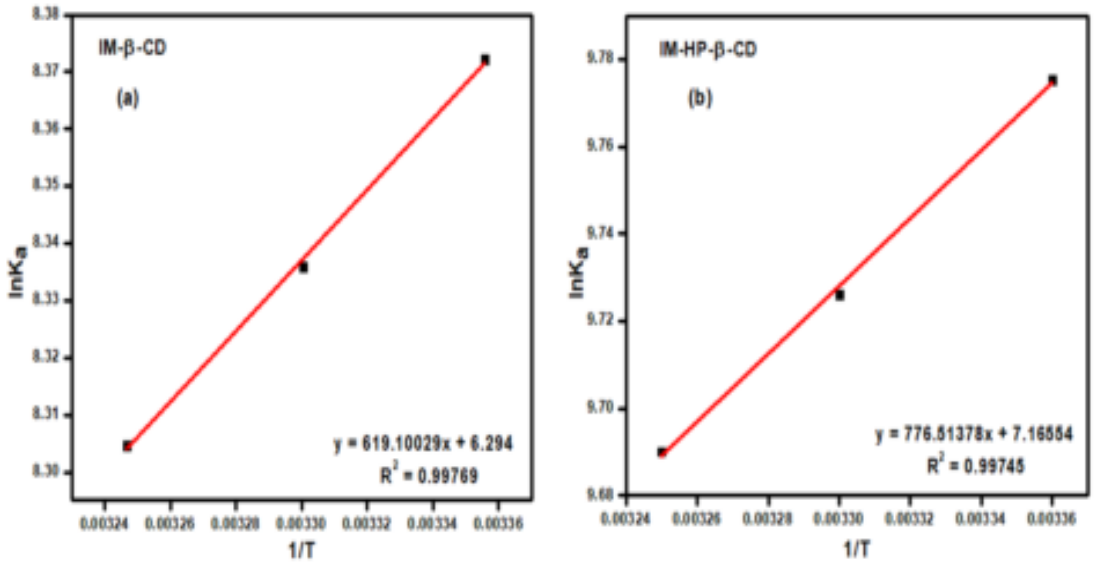

Figure 4. Plot of $\ln K_a$ vs 1/T for the interaction of IM with (a) β-CD and (b) HP-β-CD.

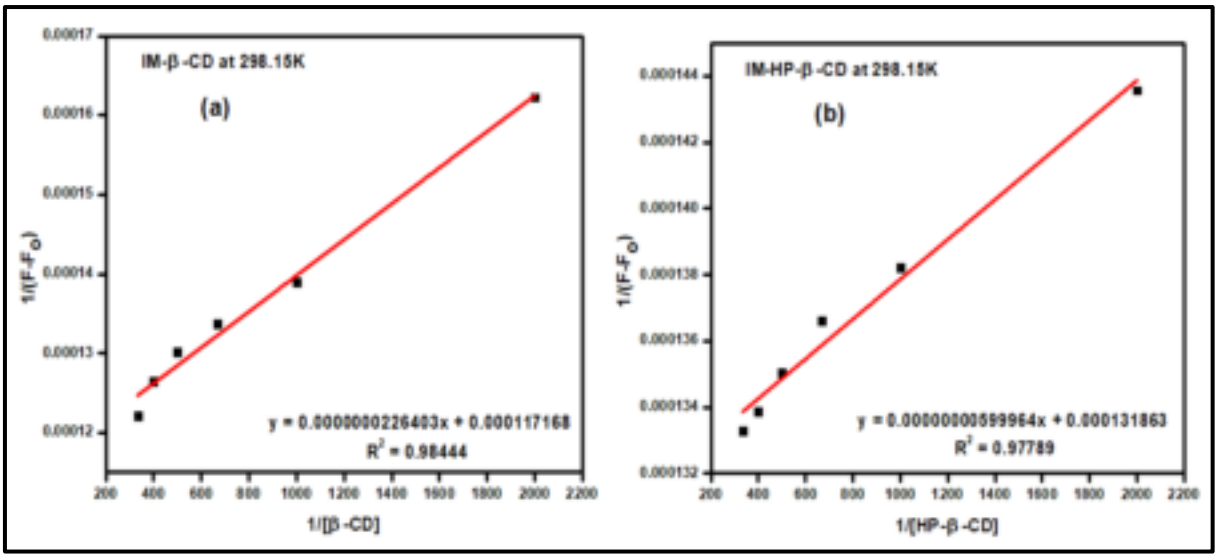

Figure 5. Benesi-Hildebrand double reciprocal plots for the effect of (a) β-CD and (b) HP-β-CD on the emission of IM (λ_{max} = 358 nm) at 298.15 K.

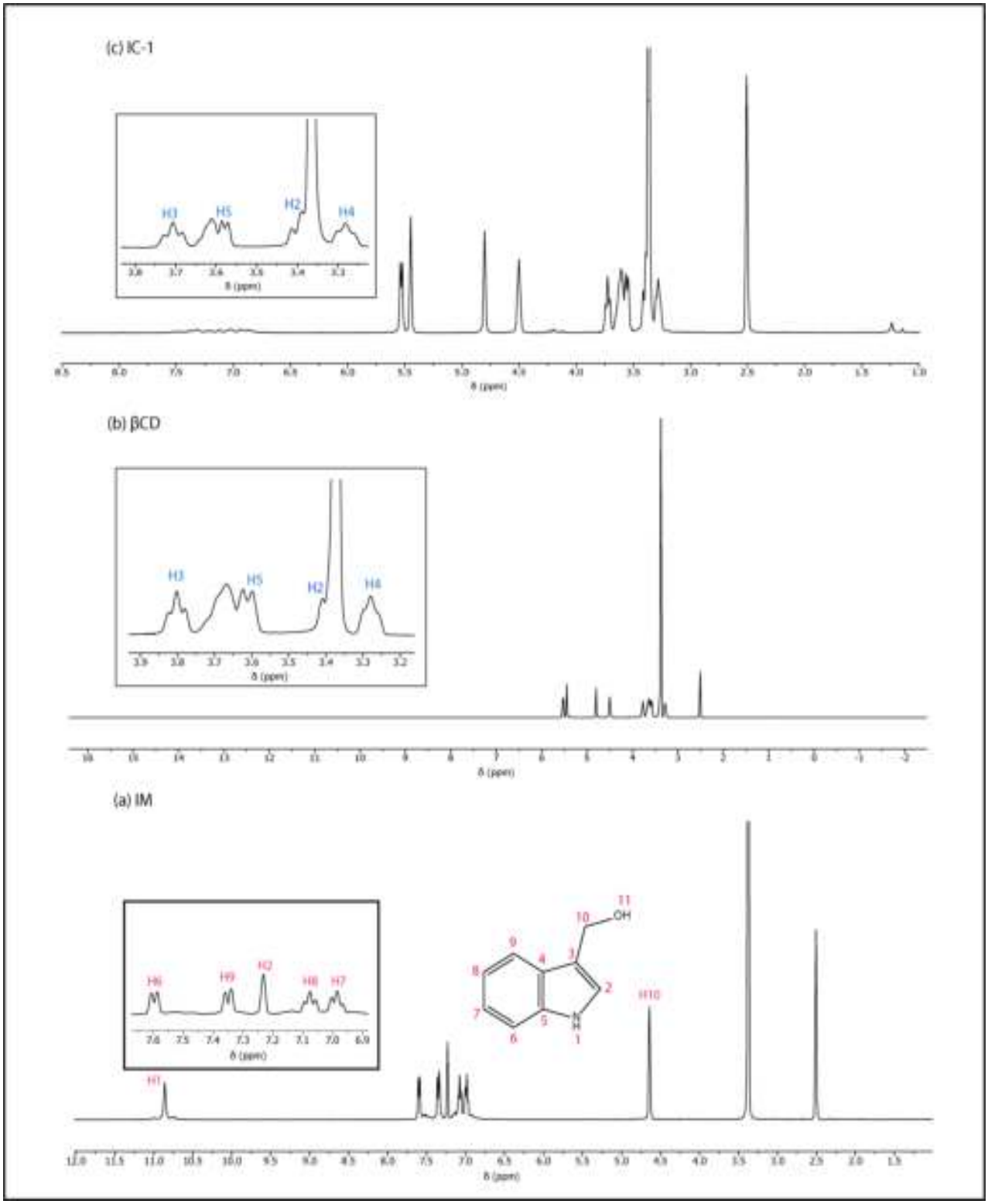

Figure 6. ^{1}H NMR spectra of (a) indole-3-methanol (IM), (b) β-CD and (c) solid inclusion complex IM-β-CD (IC1) in DMSO-d_6 at 298.15K.

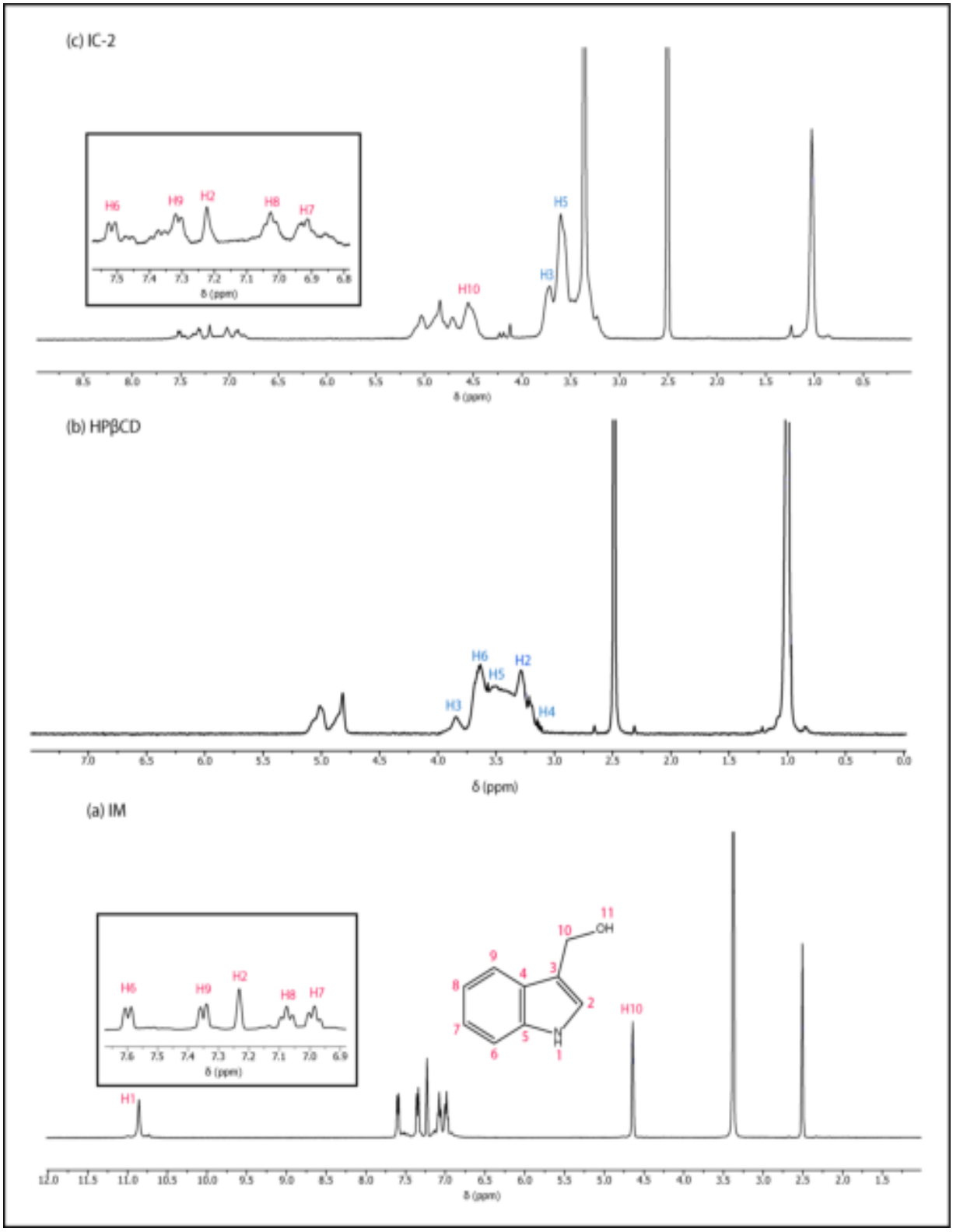

Figure 7. ^{1}H NMR spectra of (a) indole-3-methanol (IM), (b) HP-β-CD and (c) solid inclusion complex IM-HP-β-CD (IC2) in DMSO-d_6 at 298.15K.

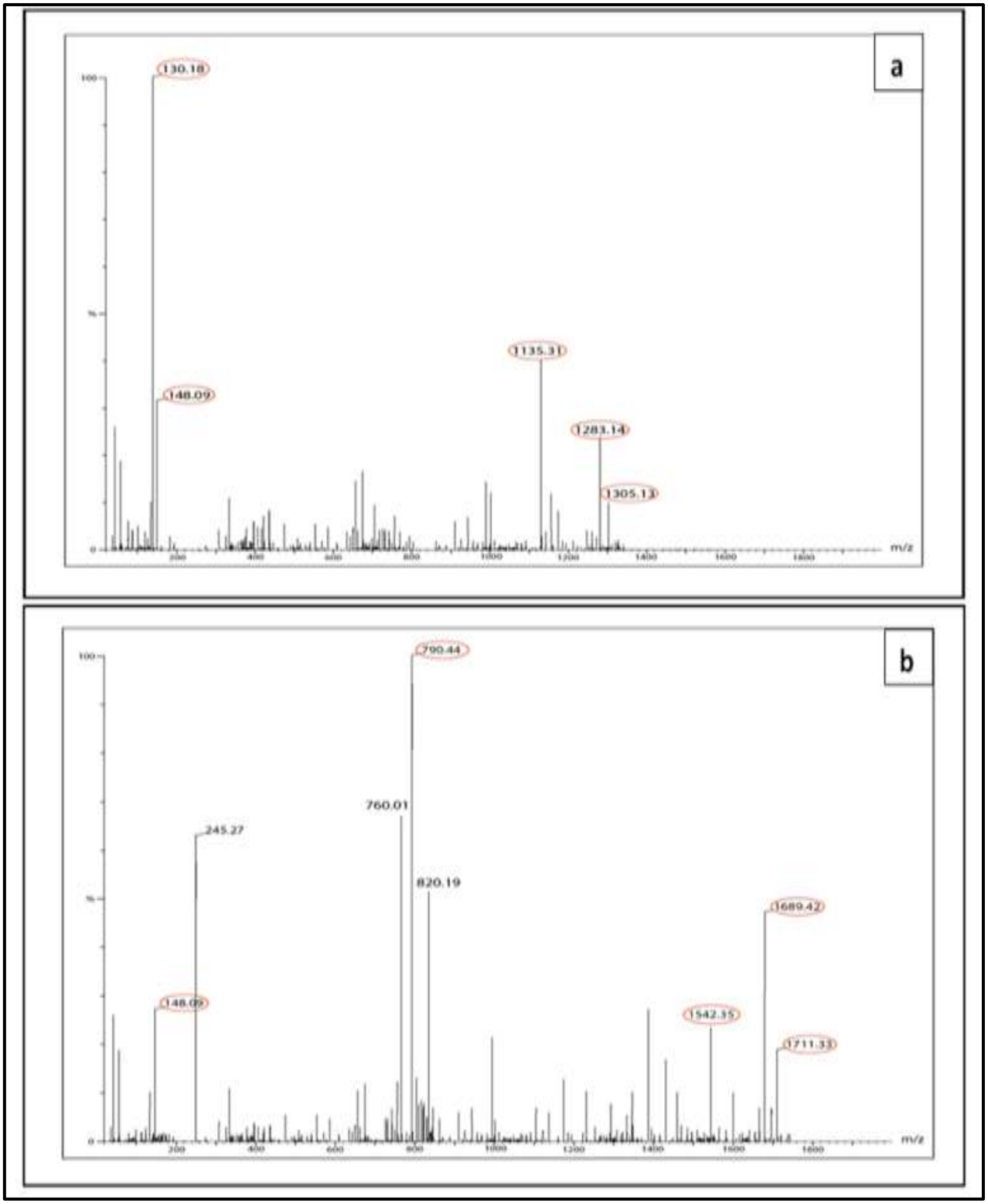

Figure 8. HRMS mass spectra of (a) IM-β-CD inclusion complex and (b) IM-HP-β-CD inclusion complex.

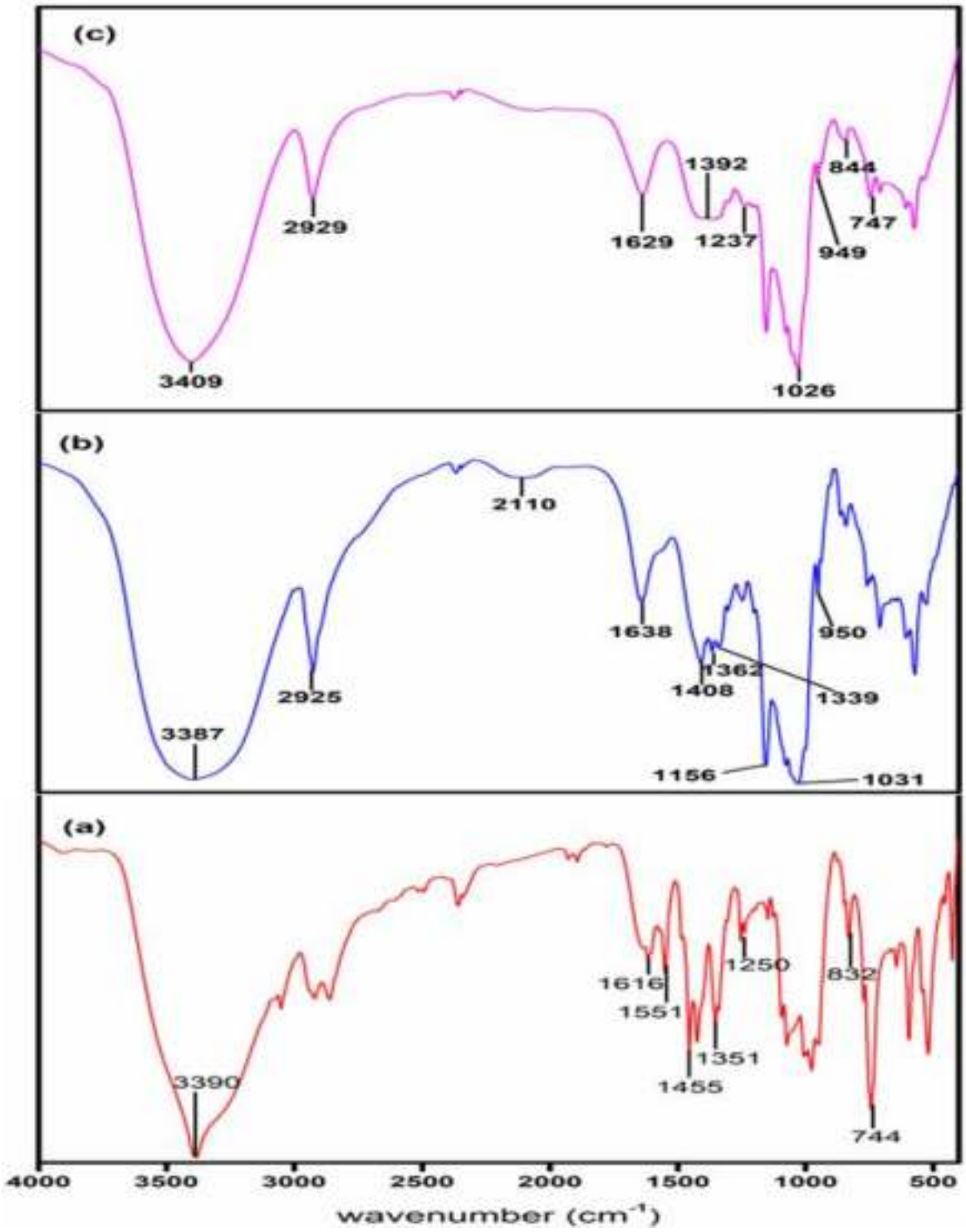

Figure 9. FT-IR spectra of (a) IM, (b) β-CD and (c) IM-β-CD inclusion complex.

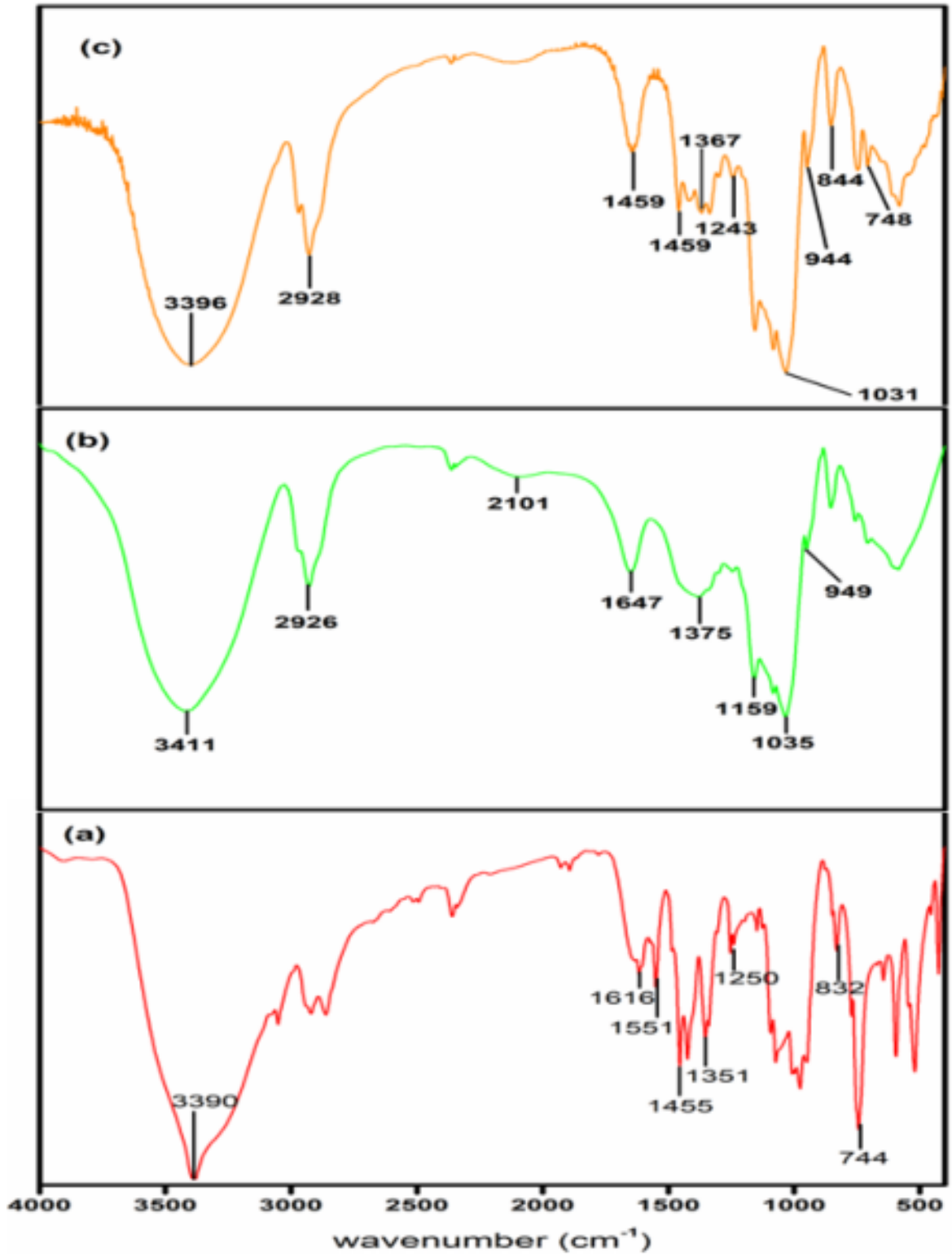

Figure 10. FT-IR spectra of (a) IM, (b) HP-β-CD and (c) IM-HP-β-CD inclusion complex.

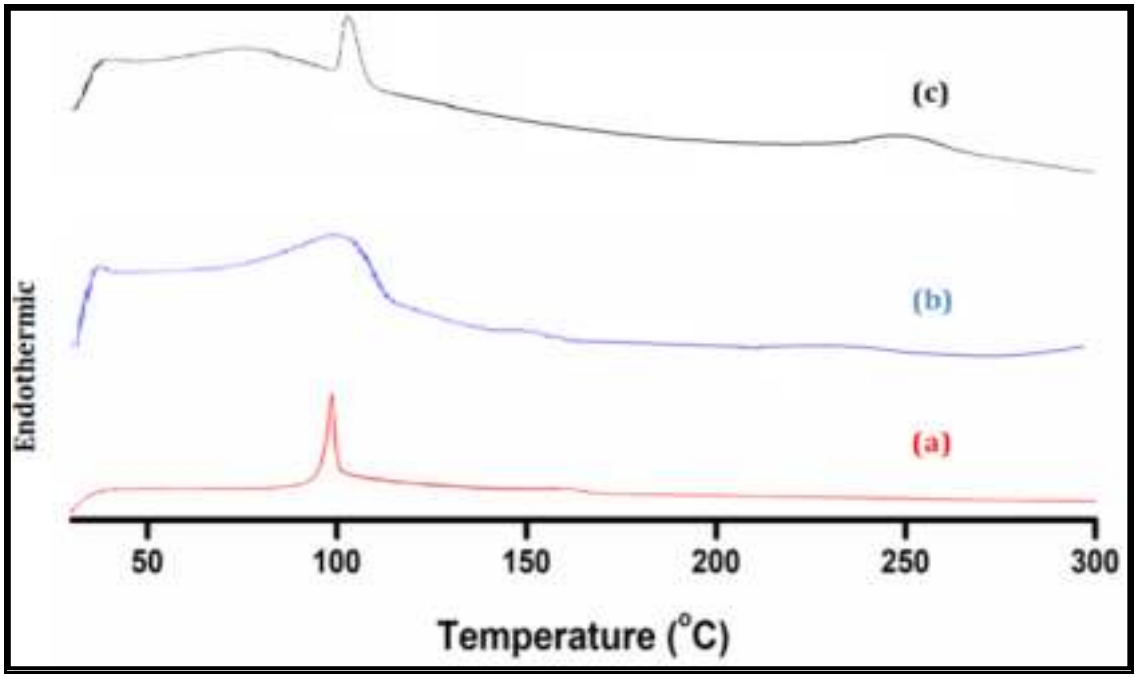

Figure 11. DSC thermograms of (a) IM, (b) β-CD and (c) IM-β-CD inclusion complex.

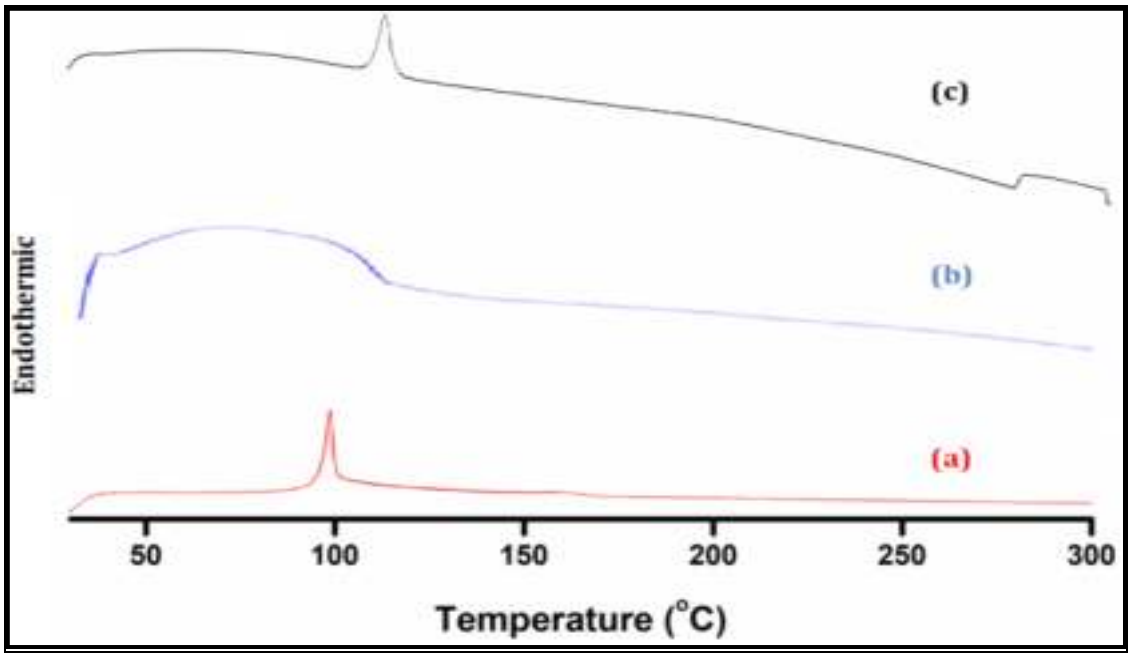

Figure 12. DSC thermograms of (a) IM, (b) HP-β-CD and (c) IM-HP-β-CD inclusion complex.

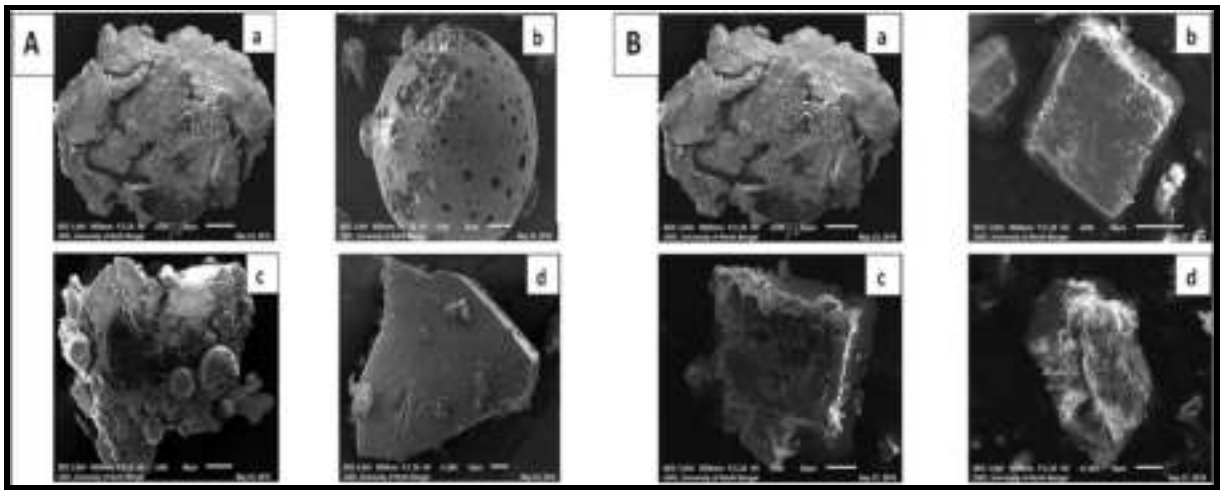

Figure 13. (A) SEM images of (a) IM, (b) HP-β-CD, (c) physical mixture of IM and HP-β-CD (PM2), (d) IM-HP-β-CD inclusion complex (IC2) ; **(B)** SEM images of (a) IM, (b) β-CD, (c) physical mixture of IM and β-CD (PM1), (d) IM-β-CD inclusion complex (IC1).

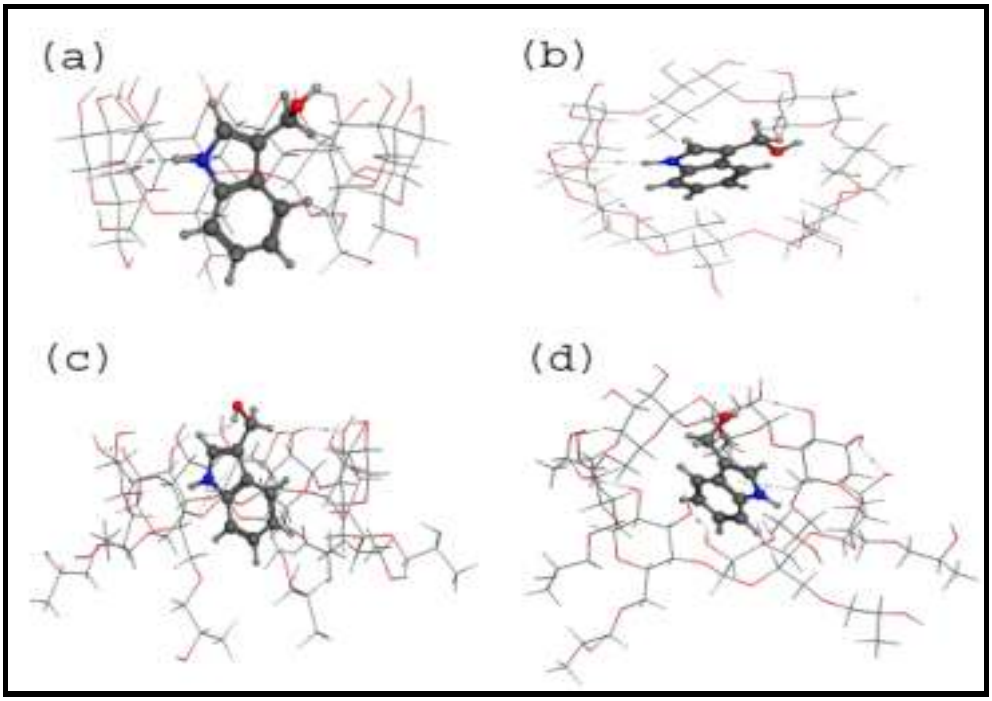

Figure 14. Binding mode of IM into β-CD (IC1) (a) side view; (b) top view, and IM into HP-β-CD (IC2) (c) side view; (d) top view.

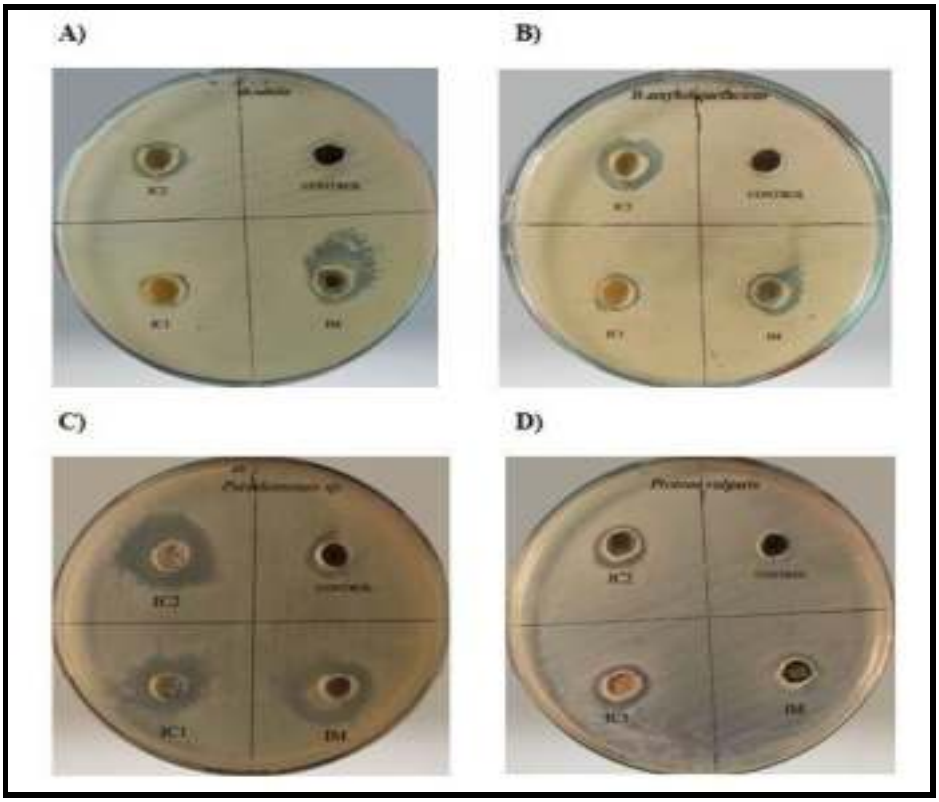

Figure 15. Antibacterial efficiency of free IM, IM-β-CD (IC1) and IM-HP-β-CD (IC2) against two gram-positive bacteria (A) *B. subtilis* (B) *B. amyloliquefaciens*, and two gram-negative bacteria (C) *Pseudomonas sp.* (D) *Proteus vulgaris*.

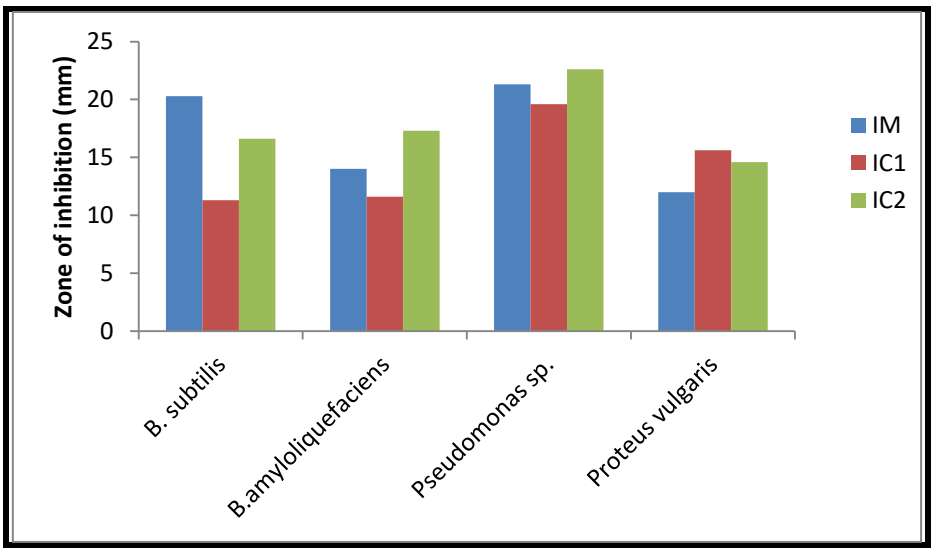

Figure 16. Zone of inhibition (mm) examined during antibacterial activity analysis of pure IM, IM-β-CD (IC1) and IM-HP-β-CD (IC2) against two gram-positive bacteria : *B. subtilis*, *B. amyloliquefaciens*, and two gram-negative bacteria : *Pseudomonas sp.*, *Proteus vulgaris*.

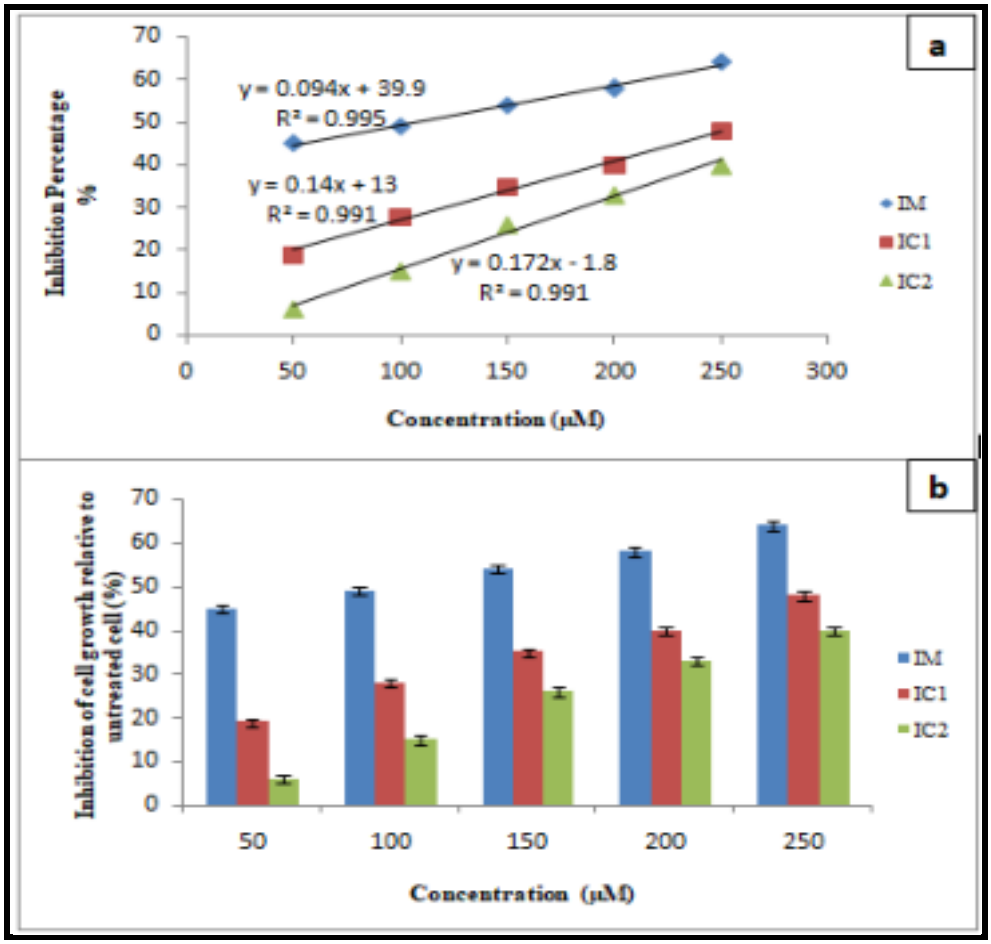

Figure 17. Cytotoxicity potential of pure IM, IM-β-CD [IC1] and IM-HP-β-CD [IC2] against normal liver cell line WRL-68 at different concentration **a)** Graph represents the linear regression and **b)** Percentage inhibition of cell growth. Data represent the mean of three replicates.

Schemes

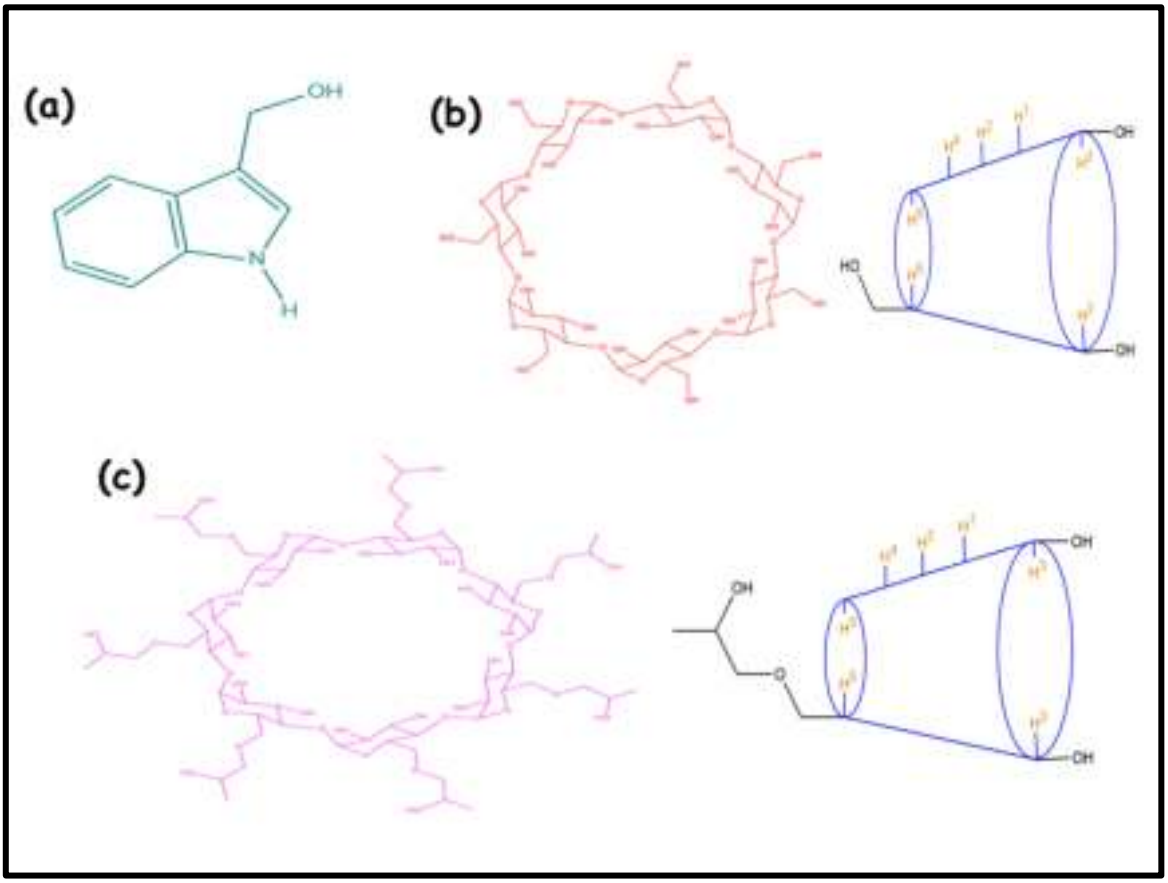

Scheme 1. Molecular Structures of **(a)** Indole-3-methanol, **(b)** β-Cyclodextrin and **(c)** Hydroxypropyl-β-Cyclodextrin.

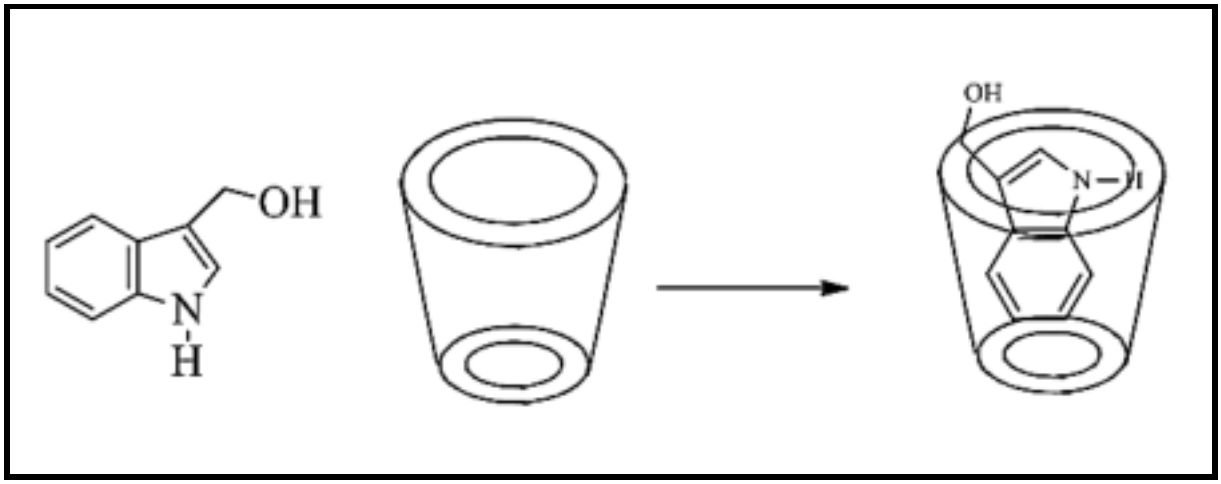

Scheme 2. Complexation of indole-3-methanol with cyclodextrin forming 1:1 inclusion complex.